Spin-polarized transport in a full magnetic pn tunnel junction

E. Comesaña, M. Aldegunde, and A. J. Garcia-Loureiro

Citation: Appl. Phys. Lett. **98**, 192507 (2011); doi: 10.1063/1.3586770
View online: https://doi.org/10.1063/1.3586770
View Table of Contents: http://aip.scitation.org/toc/apl/98/19
Published by the American Institute of Physics

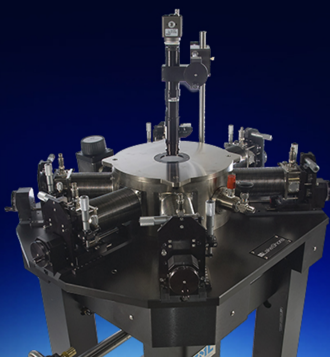
Cryogenic probe stations
for accurate, repeatable
material measurements

Reuse of AIP Publishing content is subject to the terms at: https://publishing.aip.org/authors/rights-and-permissions. Downloaded to: 193.144.79.182 on 13 November 2018, At: 00:41

Spin-polarized transport in a full magnetic pn tunnel junction

E. Comesaña,[1,a)] M. Aldegunde,[2] and A. J. Garcia-Loureiro[1]
[1]*Departamento de Electrónica e Computación, Universidade de Santiago de Compostela, 15782 Santiago de Compostela, Spain*
[2]*Centro de Supercomputación de Galicia (CESGA), 15705 Santiago de Compostela Spain*

(Received 18 November 2010; accepted 13 April 2011; published online 11 May 2011)

Simulations of the tunneling current as a function of voltage and temperature for a Zener diode where both sides are ferromagnetic have been performed. The current is evaluated as a function of the applied bias, the magnetization, and the temperature on the diode. The tunneling magnetoresistance is also analyzed. Mn doped GaAs parameters were used to simulate a highly asymmetric doped diode, which leads to a large difference on the magnetization values between the p and n sides. © *2011 American Institute of Physics*. [doi:10.1063/1.3586770]

The recent progress in developing semiconductor materials that show ferromagnetic characteristics at room temperatures is leading to a growing interest to replace charge with spin in signal processing devices. Spintronics is motivated by the belief that spin signal processing may yield advantages in terms of processing speed, power consumption, or device density.

Dilute magnetic semiconductors (DMSs) are showing good characteristics at rising temperatures and are being developed to achieve spin control at room temperature. In an optimally doped DMS the density of carriers is approximately half that of the density of magnetic ions which is usually between $x=5\%$ and $x=15\%$. The well established DMSs occur with one type of carrier. One of the most investigated materials is the III–V material (GaMn)As in which the Mn ion provides a localized spin $S=5/2$ and also contributes a hole.[1] The holes are degenerate and strongly polarized at low temperatures.[2] The ferromagnetic III–V doped materials are all p type but there is much effort to find a compatible n type ferromagnetic semiconductor.[3] Magnetic properties have been seen in a number of magnetically doped oxides, particularly ZnO, TiO_2, and SnO_2 (Refs. 4–6) all of which occur as n type semiconductors.

A pn junction of two highly degenerated semiconductors makes a Zener tunneling diode, which has many applications[7] and adding magnetic functionality would enable more devices such as magnetic switching of microwave devices. Also the understanding of the behavior of the ferromagnetic pn junction is cornerstone to the study of more complicated spin-based devices, such as magnetic bipolar transistors[8] or spin field-effect transistors.[9] Zener tunneling has been observed in a ferromagnetic-nonmagnetic (GaMn)As/GaAs heterostructure,[10] and a high spin polarization is observed optically.[11] The voltage dependence of the tunneling current in a spin-polarized Zener diode is well fitted by the theory of a nonmagnetic diode.[2] We are developing analytical[12] and numerical models[13] to study the transport in ferromagnetic Zener diodes. Our numerical simulator solves self-consistently drif-diffusion model equations, which has been extensively used to study spintronic devices.[14–16] Using these models we have predicted the dependence of the tunneling current on the mean magnetization of the system and we have evaluated the tunneling magnetoresistance (TMR) for different values of the applied bias and temperatures in a theoretical both-sided ferromagnetic diode.

The current through a tunneling diode has three components;[7] the tunneling current, the excess current, and the diffusion current. The tunneling current is expected to rise to a maximum at low voltage, about the lowest of the distances between the Fermi level and the conduction band in the n-side (ε_n/q_e) and the valence band in the p-side (ε_p/q_e). Then it falls to zero when bias increases over $(\varepsilon_n+\varepsilon_p)/q_e$, see Fig. 1. This fall in the *I-V* curve is known as negative resistance region (NRR) and is produced by the overlapping of the density of carrier functions in both p and n sides.[17] The last two components become important for higher voltages out of the range of interest in this letter.

In this letter, we show the results obtained for a full ferromagnetic GaAs diode from our numerical simulator. This numerical implementation intends to be more accurate than the analytical model because it takes into account the exact change in the tunneling barrier with the band splitting and the applied bias, see, for example, Fig. 2(b). While the analytical model was developed for temperatures near 0 K, the numerical simulator also allows us to run simulations at different temperatures. This letter offers a detailed analysis of the tunneling current and the effect of temperature and bias on the TMR, thanks to the improvement of the band spin-splitting model by adding the dependence of the spontaneous magnetization with the temperature.

The tunneling of carriers through the band gap is an important part of the carrier transport in highly doped pn

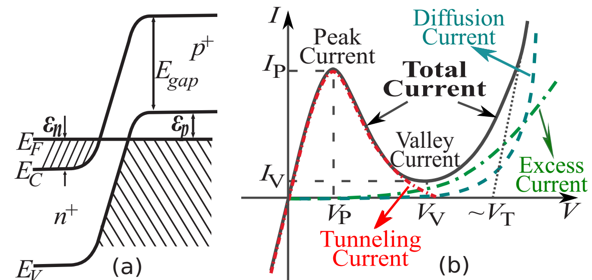

FIG. 1. (Color online) (a) Tunnel diode band diagram and (b) typical *I-V* characteristic, showing the three contributions to the total current; tunnel, excess, and diffusion currents.

[a)]Electronic mail: enrique.comesana@usc.es.

 © 2011 American Institute of Physics

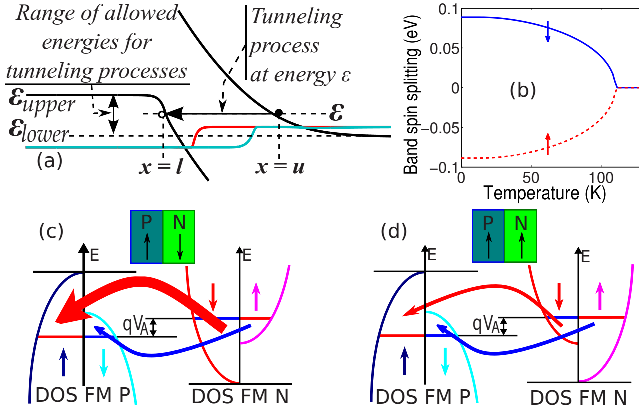

FIG. 2. (Color online) (a) Schematic representation of a tunneling process at energy ϵ. The figure shows the classical turning points, the Fermi pseudolevels and the range of allowed energies. (b) Temperature dependence of the band edge in (GaMn)As, T_C=110 K. Schematic of the spin-split bands for the antiparallel (c) and parallel (d) configuration. The arrows show the tunnel recombination processes.

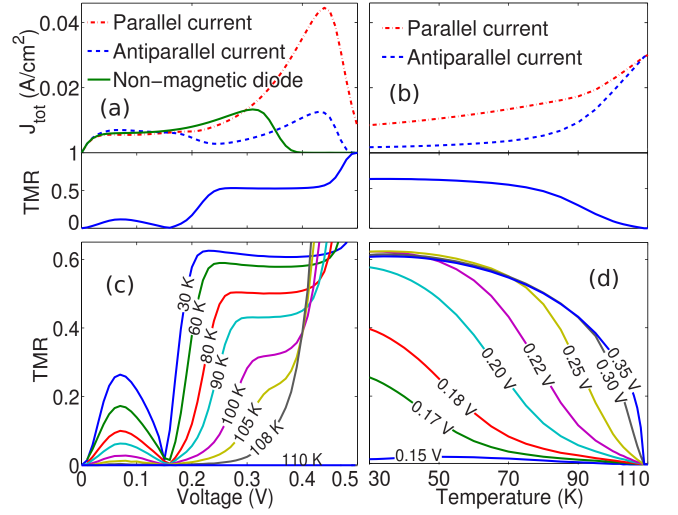

FIG. 3. (Color online) (a) Current density and TMR dependence on the bias voltage for 77 K. (b) Current density and TMR dependence on the device temperature at 0.35 V. (c) TMR variation with the temperature for different characteristic biases. (d) TMR variation with the bias for different temperatures.

junctions. There are two tunneling mechanisms; the direct transition from band to band and the trap assisted tunneling. The basic principles of the band to band tunneling were explained by Kane.[17] The tunneling probability, $\Gamma(\epsilon)$, is obtained from the WKB approximation. The tunneling density of current is described as follows:[17]

$$J_{\text{tun}} = \frac{q}{\pi\hbar}\int\int \Gamma(\epsilon)\times[f_u(\epsilon+\epsilon_t)-f_l(\epsilon+\epsilon_t)]\times\rho_t d\epsilon d\epsilon_t, \tag{1}$$

where $\rho_t=\sqrt{m_e^* m_h^*}/2\pi\hbar^2$ is the two-dimensional density of states related to the two transversal wave vectors, and f_l and f_u are the Fermi–Dirac functions evaluated using the pseudo-Fermi level of the majority carrier in the classical turning points. The tunneling current can be added to the electron and hole continuity equations as the nonlocal generation-recombination term $R_{\text{tun}}=dJ_{\text{tun}}/d\epsilon\times F$ with F the electric field.

The effect of the exchange interaction between the charge carriers and the localized magnetic moments on the energy band structure and the transport properties can be estimated by using a perturbation theory.[18] The correction of the band energies due to the exchange potential can be written as

$$E_{\mathbf{k}\sigma}=E_{be}^0+\frac{\hbar^2\mathbf{k}^2}{2m^*}-\frac{\Delta}{2}(\delta_{\sigma\uparrow}-\delta_{\sigma\downarrow}), \tag{2}$$

where $\Delta=xJ_{exch}\langle S^z\rangle$ is the band splitting. In the mean field approximation, the average spin polarization of the magnetic moments, $\langle S^z\rangle$, is given by $x\langle S^z\rangle=xSB_S(y)$, where x is the Mn ions concentration and $B_S(y)$ is the Brioullin function for the spin S.

Figure 2(b) shows the calculated band splitting of the band edge for (GaMn)As using this approach of the exchange interaction with J_{exch}^{pd}=1.4 eV, $m^*=0.5m_0$, T_C=110 K, and $S=5/2$. The band splitting disappears for temperatures over T_C at $B=0$ and rises to a maximum value for low temperatures.

When the bands edges are spin-split, there are two different characteristic energies for the occupations for each spin $\varepsilon_{\rm n}^{\sigma}=E_{Fn}-E_C^{\sigma}=E_{Fp}-E_C\pm\Delta_{\rm n}/2$ and $\varepsilon_{\rm p}^{\sigma}=E_V^{\sigma}-E_{Fp}=E_V-E_{Fp}\pm\Delta_{\rm p}/2$ with $\sigma=(\uparrow,\downarrow)$. The tunneling occurs between the two majority and the two minority bands or, if the relative magnetization of the layer is reversed, between the majority and the minority bands, see Fig. 2. We call these currents antiparallel current $I_{ap}(V)$, Fig. 2(c), and parallel current $I_p(V)$, Fig. 2(d), respectively. The tunneling recombination term is reevaluated for each spin-band obtaining four recombination terms related with the $e^{\uparrow}-h^{\downarrow}$ and the $e^{\downarrow}-h^{\uparrow}$ recombinations.

To calculate the spin splitting we assume that the total carrier concentration remains constant when the spin is polarized, $\rm n^0=n^{\uparrow}+n^{\downarrow}$ and $\rm p^0=p^{\uparrow}+p^{\downarrow}$, where $\rm n^0$ and $\rm p^0$ are the electron and hole concentrations with no spin polarization. In this letter we have made the assumption that the spin polarization ratio, defined as $P=|\rm n^{\uparrow}-n^{\downarrow}|/n^0$ or $P=|\rm p^{\uparrow}-p^{\downarrow}|/p^0$ (both are equivalent), is conserved in each device region, a valid approximation as long as the spin coherence length (several micro meter) is much larger than the depletion region width (several nano meter in our devices). Therefore, the band splitting in the depletion region will drop smoothly as the carrier concentration decreases. To study the ferromagnetic and the antiferromagnetic interactions between the p and n sides, which correspond to the antiparallel and parallel configurations, we considered that the spin flip occurs in the depletion region, in the point where the carrier concentration reaches its minimum, because in that point the carrier mediated exchange interaction has to be weaker.

If a Zener diode with both sides ferromagnetic is taken around a hysteresis loop it should show TMR $\text{TMR}=|I_p(V)-I_{ap}(V)|/[I_p(V)+I_{ap}(V)]$ because the magnetizations would be parallel at large fields and antiparallel at intermediate field value. We made calculations choosing doping levels of $N_d=2\times10^{18}$ cm^{-3} in the n-side and $N_a=3\times10^{20}$ cm^{-3} in the p-side, in a constant profile for each side. These doping levels lead to the typical carrier concentration levels in $(\rm Ga_{0.9}Mn_{0.1})As$ magnetic semiconductors, which exhibit a Curie temperature of around 110 K. The voltage dependence of I_p, I_{ap} and the TMR are shown in Fig. 3(a) for a temperature of 77 K. The simulations results are analyzed between 0

and 0.4 V, the range in which the tunneling current in the nonmagnetic diode is expected to be nonzero. Larger bias values are not considered because the ferromagnetism effects are only important for low biases.[19,20] It is worth noting that the antiparallel current is higher than the parallel current for very low biases (<0.15 V). In this case the tunneling current is controlled by the carriers with higher energy, which have similar distributions in the parallel and antiparallel configurations, and the antiparallel configuration leads to higher tunneling probabilities for low voltages. Also, the apparently high values of the TMR for biases larger 0.4 V are unphysical because the other current components will become more relevant, hiding the effect of the ferromagnetism on the tunneling current.

To analyze the dependence of the TMR on the temperature, the calculations were repeated for different temperatures between 30 and 110 K. Figure 3(b) shows the evolution of the tunneling current in the parallel and antiparallel configurations and the corresponding TMR for different temperatures. The tunneling current corresponds to a bias of 0.35 V, chosen in the middle of the NRR as we expect the TMR maximum value in this range.[12] The TMR shows saturation at low temperatures around 60% and it falls down and disappears as the temperature goes near and further of the Curie temperature ($\sim$110 K). This is what we expect from the change in the band splitting with the temperature, Fig. 2(b).

The TMR tends to saturate its value in the NRR, this can be seen in Figs. 3(c) and 3(d), where the TMR is almost constant for biases in the NRR. Figure 3(c) also shows how the TMR in the NRR acts an upper bound in the TMR evolution for low biases. In Fig. 3(d) we observe that the TMR signal is stronger for higher voltages in the NRR; however, we have to find a tradeoff between this increase and the degradation of the TMR at high biases associated to other current components. It is also worth mentioning that the parallel current always becomes larger than the antiparallel current at the same bias, $V_A \sim 0.15$ mV. At this voltage, the energy overlapping between the carrier distributions in the p and n sides reaches its maximum in the parallel configuration and therefore the lowest energy carriers start to dominate the tunneling current. In this moment, the parallel configuration begins to generate larger currents than the antiparallel one.

The results derived here will act as a guide to what should be expected in an experiment. They also intend to be a temperature and voltage parametrization of the behavior of a future device based on a ferromagnetic pn junction. The TMR becomes more intense for growing voltages and saturates in the NRR and also at low temperatures. Study of the voltage dependence of the tunneling current will give detailed information on the relative size of the spin polarization of the carriers in each band.

This work was supported by Spanish Government (Grant Nos. TIN2007-67537-C03-01 and TEC2010- 17320) and by Xunta de Galicia (Grant Nos. DXIDI09TIC001CT and INCITE08PXIB206094PR).

[1] T. Jungwirth, J. Sinova, J. Mašek, J. Kučera, and A. H. MacDonald, Rev. Mod. Phys. **78**, 809 (2006).
[2] H. Holmberg, N. Lebedeva, S. Novikov, P. Kuivalainen, M. Malfait, and V. V. Moshchalkov, Phys. Status Solidi A **204**, 791 (2007).
[3] J. Mašek, J. Kudrnovský, F. Máca, B. L. Gallagher, R. P. Campion, D. H. Gregory, and T. Jungwirth, Phys. Rev. Lett. **98**, 067202 (2007).
[4] A. Ney, V. Ney, S. Ye, K. Ollefs, T. Kammermeier, T. Kaspar, S. Chambers, F. Wilhelm, and A. Rogalev, Phys. Rev. B **82**, 041202(R) (2010).
[5] A. Serrano, E. Pinel, A. Quesada, I. Lorite, M. Plaza, L. Pérez, F. Jiménez-Villacorta, J. de La Venta, M. Martín-González, J. Costa-Krämer, J. Fernandez, J. Llopis, and M. García, Phys. Rev. B **79**, 144405 (2009).
[6] A. Espinosa, M. García-Hernández, N. Menéndez, C. Prieto, and A. de Andrés, Phys. Rev. B **81**, 064419 (2010).
[7] S. M. Sze and K. K. Ng, *Physics of Semiconductor Devices*, 3rd ed. (Wiley, New York, 2006).
[8] J. Fabian, I. Žutić, and S. Das Sarma, Appl. Phys. Lett. **84**, 85 (2004).
[9] H. Ohno, D. Chiba, F. Matsukura, T. Omiya, E. Abe, T. Dietl, Y. Ohno, and K. Ohtani, Nature (London) **408**, 944 (2000).
[10] P. Sankowski, P. Kacman, J. Majewski, and T. Dietl, Phys. Rev. B **75**, 045306 (2007).
[11] G. van der Laan, K. Edmonds, E. Arenholz, N. Farley, and B. Gallagher, Phys. Rev. B **81**, 214422 (2010).
[12] E. Comesaña and G. A. Gehring, Appl. Phys. Lett. **91**, 142510 (2007).
[13] M. Aldegunde, E. Comesaña, G. A. Gehring, and A. J. Garcia-Loureiro, *Spanish Conference on Electron Devices* (IEEE, Santiago de Compostela, 2009), p. 160.
[14] I. Žutić, J. Fabian, and S. Das Sarma, Phys. Rev. Lett. **88**, 066603 (2002).
[15] I. Žutić, J. Fabian, and S. C. Erwin, IBM J. Res. Dev. **50**, 121 (2006).
[16] M. I. Miah and E. M. Gray, Curr. Opin. Solid State Mater. Sci. **13**, 99 (2009).
[17] E. O. Kane, J. Appl. Phys. **32**, 83 (1961).
[18] N. Lebedeva and P. Kuivalainen, J. Appl. Phys. **93**, 9845 (2003).
[19] E. Tsymbal, K. Belashchenko, J. Velev, S. Jaswal, M. Vanschilfgaarde, I. Oleynik, and D. Stewart, Prog. Mater. Sci. **52**, 401 (2007).
[20] G. Chen, F. Zeng, and F. Pan, Appl. Phys. Lett. **95**, 232508 (2009).